J. Fluid Mech. (1988), *vol.* 194, *pp.* 563–579
Printed in Great Britain

Effects of soluble and insoluble surfactants on the motion of drops

By H. N. OĞUZ† AND S. S. SADHAL‡

† Department of Mechanical Engineering, The Johns Hopkins University, Baltimore, MD 21218, USA

‡ Department of Applied Mathematics and Theoretical Physics, University of Cambridge, Silver Street, Cambridge CB3 9EW, UK

(Received 8 April 1987 and in revised form 8 January 1988)

The fluid dynamics of moving drops in the presence of a soluble surfactant and an insoluble impurity is examined in detail. The main purpose of this analysis is to establish a fairly general theory that agrees with experimental measurements. Particular attention is paid to situations involving a stagnant cap which arise when low-solubility surfactants are present. Earlier theories on stagnant caps have not satisfactorily explained the experimental results and a two-impurity model is therefore proposed. The analysis is carried out semi-analytically using a matched asymptotic analysis of the Proudman–Pearson type for weakly inertial flows. The results seem to be in good agreement with the available data at a Péclet number of about 700 for the soluble surfactant. In particular the predicted flow field within the drop is found to be consistent with the experimental measurements of Horton. The concentration profiles graphically exhibit the physical phenomena involved in the mass transport. Another new result is the analytical expression for the drag force corrected up to $O(Re)$ for the case involving only the insoluble surfactant.

1. Introduction

The motion of spherical drops or bubbles has been observed to be affected considerably by the impurity levels of the fluids involved. An interesting aspect of this phenomenon is that the surface-active agents usually collect at the surface of the drop where they often form a stagnant cap around the rear stagnation point. The presence of such a cap makes a considerable change in the flow pattern inside the drop. The main focus of the present analysis is to establish a suitable theory that agrees well with the experimental observations of the flow field.

The early experiments by Bond & Newton (1927) have shown that for very small drops and bubbles the drag force undergoes a sharp transition as the size is varied. They observed that, below some critical radius, air bubbles behaved like solid spheres. They tried to explain this phenomenon by the presence of impurities and found a correlation between the surface tension and the critical radius.

Later experimental studies on the effect of surfactants by Savic (1953), Garner & Skelland (1955), Elzinga & Banchero (1961), Griffith (1962), Horton, Fritsch & Kintner (1965) and Huang & Kintner (1969) revealed some interesting phenomena. It is observed that as the surfactants concentrate at the surfaces of drops and bubbles they tend to decrease surface tension with concentration. These impurities are transported to the rear of the drop or bubble by the motion of the interface,

where they form a surface-tension gradient that may immobilize all of the interface or a portion of it, like a solid cap.

Mathematical modelling and theoretical studies by Frumkin & Levich (1947), Dukhin & Deryagin (1961), Newman (1967), Wasserman & Slattery (1969), Schechter & Farley (1963), Saville (1973), Lucassen & Giles (1975), and LeVan & Newman (1976) have usually led to a common analytical difficulty: a singularity at the rear axis. In the case of a high ratio of convective to diffusive transport (i.e. large Péclet number) a cap is formed and a further difficulty arises from the mixed boundary-value problem. This is because the boundary conditions change character at the interface which must have no-slip on the cap but mobility on the remaining portion of the same interface. This mixed boundary condition has been numerically treated by Savic (1953), and Davis & Acrivos (1966), and an asymptotic analysis has been carried by Harper (1973, 1982). To account for bulk diffusion LeVan & Newman (1976) solved the convection–diffusion equation by using a finite-difference formulation but they did not consider the effect of the surfactant on the velocity field. Some years ago Sadhal & Johnson (1983) gave an exact solution to the mixed boundary-value problem for the case of insoluble surfactants forming a cap of any specified angle. The cases of soluble surfactants in the continuous phase have been treated by Holbrook & LeVan (1983*a*,*b*) who used the collocation method to solve the convection–diffusion problem for high Péclet number. Their results showed an appreciable amount of interfacial velocity retardation but it was not enough to show a well-defined cap.

In the area of surface shear and surface dilational effects (see Scriven 1960) an analytical application to drops and bubbles was given by LeVan (1981). Agrawal & Wasan (1979) carried out an analysis to combine the surface viscosity effects and weak surfactant effects. Slattery *et al.* (1980) proposed a technique for measuring surface viscosities: they carried out measurements on a spinning drop to obtain the surface viscosities. In a review paper, Dussan V. (1982) critically examined the surface viscometer developed by Poskanzer & Goodrich (1975).

Despite the large number of investigations in the field there are still unanswered questions about the fluid dynamics in relation to the cap. Horton's (1960) experiments, which were reported by Huang & Kintner (1969), show that the centre of the internal vortex in the drop shifts towards the front of the drop as the cap size increases. Harper (1982) used an asymptotic analysis for small caps to predict the flow field inside the drop. His comparison with Horton's (1960) experimental data gave good agreement for small caps but it became poorer as the cap size was increased. It was felt that the disagreement arose from the lack of validity of the solution, rather than the model. However, the exact solution of Sadhal & Johnson (1983), which is valid for all cap sizes in the case of an insoluble surfactant, also failed to give good agreement. In an effort to find an explanation, a two-impurity model is proposed here. One impurity is totally insoluble in both the drop and the surrounding fluid. The other is soluble in both of these phases but may be surface-active. The insoluble one may be composed of very small dust-like particles that usually collect at the drop interface. In the case where the drop translates, owing to the buoyant forces the particles are convected to the rear where they form a stagnant cap at the interface (see figure 1). The presence of the soluble impurity will further slow down the interface by creating a surface-tension gradient along the 'clean' part of the interface.

The assumption of the existence of a stagnant cap limits the flow field to small Reynolds numbers since at high Reynolds numbers the separation of the boundary

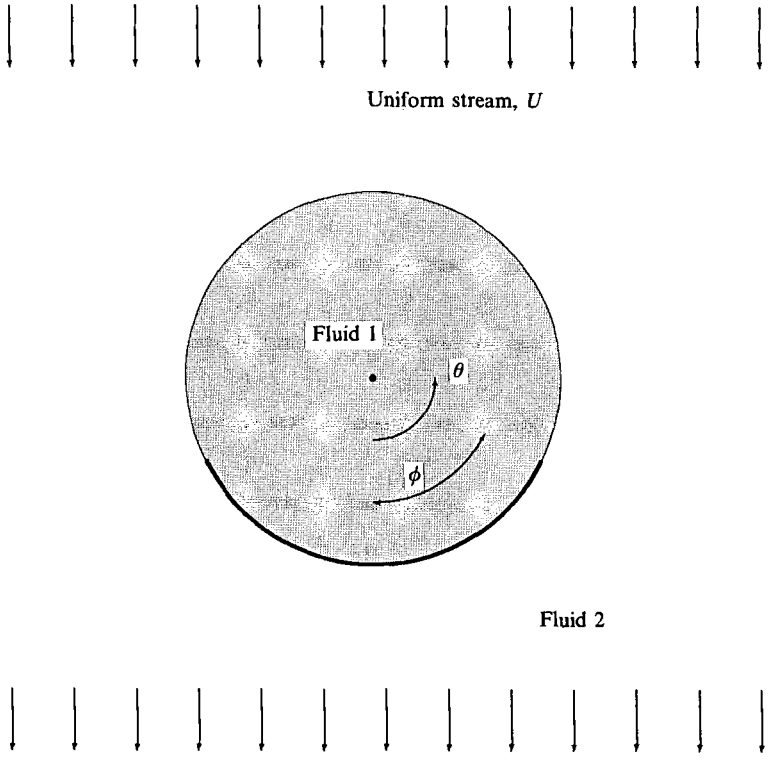

FIGURE 1. A schematic of a compound multiphase drop with a spherical cap of an angle ϕ.

layer could change the form of the cap considerably. The normal surface-tension forces are considered to be large enough that the drop can be assumed to be spherical. This assumption (i.e. small capillary numbers) is usually a fairly good one in the case of small Reynolds numbers for most fluids. For a small Reynolds number the flow field can be determined as a series expansion of unknown coefficients. The inertial effects can be taken into account by an Oseen-type solution.

In the next section the general problem is stated and a numerical solution is presented for a fairly general case.

2. Statement of the problem

With the above conditions, the governing equations can be written in a dimensionless form and a spherical coordinate system is appropriate. Here the drop is referred as fluid 1 and the surrounding phase as fluid 2.

Continuity

$$\nabla \cdot \boldsymbol{u}_i = 0 \quad (i = 1, 2); \tag{1}$$

Momentum

$$Re_i \boldsymbol{u}_i \cdot \nabla \boldsymbol{u}_i = -\nabla p_i + \mu_i \nabla^2 \boldsymbol{u}_i \quad (i = 1, 2 \text{ no sum}), \tag{2}$$

Surfactant transport in the bulk phase

$$\tfrac{1}{2} Pe_i \nabla \cdot \boldsymbol{u}_i c_i = \nabla^2 c_i \quad (i = 1, 2 \text{ no sum}). \tag{3}$$

The boundary and interface conditions are as follows:

far-field: uniform velocity; uniform surfactant concentration;

interface: zero normal velocity; continuity of tangential velocity, continuity of shear stress for $\phi \leqslant \theta \leqslant \pi$, zero tangential velocity for $0 \leqslant \theta \leqslant \phi$; surfactant mass balance; kinetics of adsorption.

These conditions will be written in mathematical form in the next section.

3. Solution

Now it is convenient to introduce the Stokes stream functions in the spherical coordinate system:

$$u_\theta^{(i)} = -\frac{1}{r\sin\theta}\frac{\partial\psi^{(i)}}{\partial r}; \quad u_r^{(i)} = \frac{1}{r^2\sin\theta}\frac{\partial\psi^{(i)}}{\partial\theta}. \tag{4}$$

With the continuity conditions satisfied the problem can be posed in the following manner:

momentum

$$\mathrm{L}_{-1}^2(\psi^{(i)}) = \frac{Re_i}{r^2\sin\theta}\left(\psi_\theta^{(i)}\frac{\partial}{\partial r} - \psi_r^{(i)}\frac{\partial}{\partial\theta} + 2\cot\theta\psi_r^{(i)} - 2\frac{\psi_\theta^{(i)}}{r}\right)\mathrm{L}_{-1}(\psi^{(i)}), \tag{5}$$

where

$$\mathrm{L}_{-1} \equiv \frac{\partial^2}{\partial r^2} + \frac{\sin\theta}{r^2}\frac{\partial}{\partial\theta}\left(\frac{1}{\sin\theta}\frac{\partial}{\partial\theta}\right);$$

surfactant transport in the bulk phases

$$\nabla^2 c_i = \tfrac{1}{2}Pe_i\left[\frac{u_\theta^{(i)}}{r}\frac{\partial c_i}{\partial\theta} + u_r^{(i)}\frac{\partial c_i}{\partial r}\right], \tag{6}$$

where

$$\nabla^2 \equiv \frac{1}{r^2}\frac{\partial}{\partial r}r^2\frac{\partial}{\partial r} + \frac{1}{r^2\sin\theta}\frac{\partial}{\partial\theta}\left(\sin\theta\frac{\partial}{\partial\theta}\right).$$

The boundary/interface conditions can now be written as

$$\psi^{(2)} = \tfrac{1}{2}r^2\sin^2\theta \quad \text{as } r\to\infty, \tag{7}$$

$$c_2 = 1 \quad \text{as} \quad r\to\infty, \tag{8}$$

$$\psi^{(2)}|_{r=1} = \psi^{(1)}|_{r=1} = 0, \tag{9}$$

$$\left.\frac{\partial\psi^{(2)}}{\partial r}\right|_{r=1} = \left.\frac{\partial\psi^{(1)}}{\partial r}\right|_{r=1}, \tag{10}$$

$$\frac{\mathrm{d}\Gamma}{\mathrm{d}\theta} = \frac{E\ddot{o}}{18F^*\sin\theta}\frac{\partial}{\partial r}\left[\frac{1}{r^2}\frac{\partial}{\partial r}\left(\psi^{(2)} - \frac{\mu_1}{\mu_2}\psi^{(1)}\right)\right]_{r=1}, \quad \phi \leqslant \theta \leqslant \pi, \tag{11a}$$

$$\left.\frac{\partial\psi^{(2)}}{\partial r}\right|_{r=1} = \left.\frac{\partial\psi^{(1)}}{\partial r}\right|_{r=1} = 0, \quad 0 \leqslant \theta \leqslant \phi, \tag{11b}$$

$$\frac{1}{Pe_1}\frac{\partial c_1}{\partial r} - \frac{1}{Pe_2}\frac{\partial c_2}{\partial r} = K\frac{1}{\sin\theta}\frac{\mathrm{d}}{\mathrm{d}\theta}(\sin\theta\Gamma u_\theta)|_{r=1}, \tag{12}$$

$$\Gamma = c_1|_{r=1}/\beta = c_2|_{r=1}, \tag{13}$$

with $$\Gamma = \frac{\sigma_0 - \sigma}{\sigma_0 - \sigma_\infty}.$$

Here ϕ is defined as the cap angle. The following dimensionless constants are involved in the problem: $Re_i = \rho_i UR/\mu_i$, $Pe_i = 2UR/D_i$, $E\ddot{o} = 4R^2 g\Delta\rho/\Delta\sigma$, $K = K_1/2R$. Here U is the velocity of the drop and R its radius, μ is the viscosity, D the diffusivity of the surfactant in the bulk phase, $\Delta\rho = |\rho_2 - \rho_1|$ the density difference, $\Delta\sigma = \sigma_0 - \sigma_\infty$ the surface-tension difference due to contamination in the absence of motion, K_1 pertains to the kinetics of adsorption and F^* is the drag force non-dimensionalized with respect to the Stokes drag, $6\pi\mu_2 UR$. Here, the kinetics of the interface is described by the linear relationship between the bulk and the surface concentrations. This, in fact, implies that there is no adsorption barrier. This type of simplified model is adequate for dilute systems, as considered here. The volumetric concentration c is non-dimensionalized by the concentration at infinity c_∞, and β is the equilibrium ratio of the concentrations at the interface. The velocity U is determined by the drag force in a constant gravity field. Since the drag is a function of the contamination, U has to be updated with every iteration of the numerical calculation of the solute concentration. The drag coefficient F^* appears in (11*a*) because of the scaling with respect to a variable velocity [$U = E\ddot{o}\Delta\sigma/(18\mu_2 F^*)$] in a constant gravity field. Such a scaling appears to be suitable for comparisons with experiments, which are generally conducted in a constant-g environment. The surface diffusion effects have been neglected in (12) because these are generally considered to be weak.

A series solution with unknown coefficients can be obtained for the fluid mechanics by using the Reynolds number Re_2 as a perturbation parameter. The first-order approximation is the Stokes solution and the second-order one is the Oseen-type solution obtained by singular perturbation. The stream-function expansions, which satisfy every boundary/interface conditions except the continuity of shear stress and the zero normal velocity, can be written as follows (see Van Dyke 1975).

In the continuous phase (fluid 2) the outer solution is

$$\psi^{(2)} = \tfrac{1}{2}r^2 \sin^2\theta - \frac{1}{2}\frac{A}{Re}(1+\cos\theta)[1 - e^{-\frac{1}{2}Rer(1-\cos\theta)}]. \tag{14}$$

The detailed derivation of this is given in the Appendix. The inner solution for the continuous phase is

$$\begin{aligned}\psi^{(2)} = {} & \frac{1}{2}\left(2r^2 - Ar + \frac{B}{r}\right)C_2^{-\frac{1}{2}}(\cos\theta) - \tfrac{1}{4}G' \sum_{k=2}^{\infty} C_k[r^{-k+2} - r^{-k}]C_{k+1}^{-\frac{1}{2}}(\cos\theta) \\ & + \sum_{k=2}^{\infty} S_k^{(0)}[r^{-k+2} - r^{-k}]C_{k+1}^{-\frac{1}{2}}(\cos\theta) \\ & + Re\tfrac{1}{8}A\left[\frac{1}{2}\left(2r^2 - A'r + \frac{B'}{r}\right)C_2^{-\frac{1}{2}}(\cos\theta) - \tfrac{1}{4}G' \sum_{k=1}^{\infty} C_k[r^{-k+2} - r^{-k}]C_{k+1}^{-\frac{1}{2}}(\cos\theta)\right. \\ & - \frac{1}{2}\left(2r^2 - Ar - \frac{B}{r} + C + \frac{D}{r^2}\right)C_3^{-\frac{1}{2}}(\cos\theta) + \tfrac{1}{4}E \sum_{k=1}^{\infty} R_k[r^{-k+2} - r^{-k}]C_{k+1}^{-\frac{1}{2}}(\cos\theta) \\ & \left. + \sum_{k=2}^{\infty} S_k^{(1)}[r^{-k+2} - r^{-k}]C_{k+1}^{-\frac{1}{2}}(\cos\theta)\right].\end{aligned} \tag{15}$$

For the dispersed phase (fluid 1) the stream function may be written as

$$\begin{aligned}\psi^{(1)} &= \tfrac{1}{2}G(r^4-r^2)C_2^{-\frac{1}{2}}(\cos\theta)-\tfrac{1}{4}G'\sum_{k=2}^{\infty}C_k[r^{k+3}-r^{k+1}]C_{k+1}^{-\frac{1}{2}}(\cos\theta)\\ &+\sum_{k=2}^{\infty}S_k^{(0)}[r^{k+3}-r^{k+1}]C_{k+1}^{-\frac{1}{2}}(\cos\theta)\\ &+Re\tfrac{1}{8}A\left[\tfrac{1}{2}G'(r^4-r^2)C_2^{-\frac{1}{2}}(\cos\theta)-\tfrac{1}{4}G'\sum_{k=1}^{\infty}C_k[r^{k+3}-r^{k+1}]C_{k+1}^{-\frac{1}{2}}(\cos\theta)\right.\\ &-\tfrac{1}{2}E(r^5-r^3)C_3^{-\frac{1}{2}}(\cos\theta)+\tfrac{1}{4}E\sum_{k=1}^{\infty}R_k[r^{k+3}-r^{k+1}]C_{k+1}^{-\frac{1}{2}}(\cos\theta)\\ &\left.+\sum_{k=2}^{\infty}S_k^{(1)}[r^{-k+2}-r^{-k}]C_{k+1}^{-\frac{1}{2}}(\cos\theta)\right].\end{aligned}\tag{16}$$

Here $C_{n+1}^{-\frac{1}{2}}(\cos\theta)$ is the Gegenbauer polynomial of order $n+1$ and degree $-\frac{1}{2}$. The sets of constants C_k and R_k arise from the cap condition due to the insoluble impurity. The set $S_k^{(0)}$ and $S_k^{(1)}$ are the effects of the soluble surfactant. With the asymptotic matching of the inner and the outer solutions, a uniformly valid composite solution may be written in the following form for the continuous phase:

$$\begin{aligned}\psi^{(2)} &= -\frac{1}{2}\frac{A}{Re}(1+\cos\theta)[1-e^{-\frac{1}{2}Re\,r(1-\cos\theta)}]\\ &+\frac{1}{2}\left(2r^2+\frac{B}{r}\right)C_2^{-\frac{1}{2}}(\cos\theta)-\tfrac{1}{4}G'\sum_{k=2}^{\infty}C_k[r^{-k+2}-r^{-k}]C_{k+1}^{-\frac{1}{2}}(\cos\theta)\\ &+\sum_{k=2}^{\infty}S_k[r^{-k+2}-r^{-k}]C_{k+1}^{-\frac{1}{2}}(\cos\theta)\\ &+Re\tfrac{1}{8}A\left[\frac{1}{2}\left(-A'r+\frac{B'}{r}\right)C_2^{-\frac{1}{2}}(\cos\theta)-\tfrac{1}{4}G'\sum_{k=1}^{\infty}C_k[r^{-k+2}-r^{-k}]C_{k+1}^{-\frac{1}{2}}(\cos\theta)\right.\\ &\left.-\frac{1}{2}\left(-Ar-\frac{B}{r}+C+\frac{D}{r^2}\right)C_3^{-\frac{1}{2}}(\cos\theta)+\tfrac{1}{4}E\sum_{k=1}^{\infty}R_k[r^{-k+2}-r^{-k}]C_{k+1}^{-\frac{1}{2}}(\cos\theta)\right].\end{aligned}\tag{17}$$

In this composite solution the sets of constants $S_k^{(0)}$ and $S_k^{(1)}$ have been combined into a single set $S_k(Re)$ so that

$$S_k(Re)=S_k^{(0)}+Re\,\tfrac{1}{8}A\,S_k^{(1)}+O(Re^2).\tag{18}$$

This is done because these constants have to be obtained by solving the mass transfer equations, which are left unperturbed. The reason for not perturbing the mass transfer equations is that for the convective transport we have to use a uniformly valid velocity field to $O(Re)$ (equation (17)) which no longer has the simple linear dependence on Re that we have in the inner solution given by (15). Since we are solving the mass transfer equations numerically, it is better not to perturb them at all. Furthermore, the perturbation approach could raise the question of uniform validity of the concentration profile.

At this point we also modify the stream function in the dispersed phase so that

$$\psi^{(1)} = \tfrac{1}{2}G(r^4-r^2)C_2^{-\frac{1}{2}}(\cos\theta) - \tfrac{1}{4}G' \sum_{k=2}^{\infty} C_k[r^{k+3}-r^{k+1}]C_{k+1}^{-\frac{1}{2}}(\cos\theta)$$
$$+ \sum_{k=2}^{\infty} S_k[r^{k+3}-r^{k+1}]C_{k+1}^{-\frac{1}{2}}(\cos\theta)$$
$$+ Re\,\tfrac{1}{8}A\left[\tfrac{1}{2}G'(r^4-r^2)C_2^{-\frac{1}{2}}(\cos\theta) - \tfrac{1}{4}G' \sum_{k=1}^{\infty} C_k[r^{k+3}-r^{k+1}]C_{k+1}^{-\frac{1}{2}}(\cos\theta)\right.$$
$$\left. - \tfrac{1}{2}E(r^5-r^3)C_3^{-\frac{1}{2}}(\cos\theta) + \tfrac{1}{4}E \sum_{k=1}^{\infty} R_k[r^{k+3}-r^{k+1}]C_{k+1}^{-\frac{1}{2}}(\cos\theta)\right].$$

The constants that satisfy the matching conditions and all the boundary and interface conditions are given by

$$A' = \frac{2\mu_2+3\mu_1}{\mu_2+\mu_1}, \quad B' = \frac{\mu_1}{\mu_2+\mu_1}, \quad G' = \frac{\mu_2}{\mu_2+\mu_1},$$
$$A = A' + \tfrac{1}{2}G'C_1 - 2S_1, \quad B = B' + \tfrac{1}{2}G'C_1 - 2S_1, \quad G = G' - \tfrac{1}{2}G'C_1 + 2S_1,$$
$$E = \frac{16-3A+B}{10(1+\mu_1/\mu_2)}, \quad D = 1-E, \quad C = -2B-D.$$

Here, since many of the constants contain S_1, they too have Re dependence in the same manner as S_1 does.

In the above solution the sets C_k, R_k and S_k are obtained by the application of the cap condition (11a,b). This gives the following sets of dual series equations:

$$\left.\begin{aligned} \sum_{k=1}^{\infty} C_k T_k^{-1}(\cos\theta) &= \sin\theta, \quad 0 \leqslant \theta \leqslant \phi, \\ \sum_{k=1}^{\infty} (2k+1)C_k T_k^{-1}(\cos\theta) &= 0, \quad \phi \leqslant \theta \leqslant \pi, \end{aligned}\right\} \tag{19}$$

$$\left.\begin{aligned} \sum_{k=1}^{\infty} R_k T_k^{-1}(\cos\theta) &= \sin\theta\cos\theta, \quad 0 \leqslant \theta \leqslant \phi, \\ \sum_{k=1}^{\infty} (2k+1)R_k T_k^{-1}(\cos\theta) &= 0, \quad \phi \leqslant \theta \leqslant \pi, \end{aligned}\right\} \tag{20}$$

$$\left.\begin{aligned} \sum_{k=1}^{\infty} S_k T_k^{-1}(\cos\theta) &= 0, \quad 0 \leqslant \theta \leqslant \phi, \\ \sum_{k=1}^{\infty} (2k+1)S_k T_k^{-1}(\cos\theta) &= \frac{9F^*}{E\ddot{o}(1+\mu_1/\mu_2)}\frac{d\Gamma}{d\theta}, \quad \phi \leqslant \theta \leqslant \pi, \end{aligned}\right\} \tag{21}$$

where $T_k^{-1}(\cos\theta)$ is related to Legendre polynomials as follows:

$$T_k^{-1} = \frac{\sin\theta}{k(k+1)}P_k'(\cos\theta).$$

The solution to (19) has been given by Sadhal & Johnson (1983) as

$$\left.\begin{aligned} C_k &= -\frac{1}{\pi}\left\{\sin(k+2)\phi - \sin k\phi + \sin(k+1)\phi - \sin(k-1)\phi \right.\right. \\ &\quad \left.\left. -2\left[\frac{\sin(k+2)\phi}{k+2} + \frac{\sin(k-1)\phi}{k-1}\right]\right\} \quad (k \neq 1), \\ C_1 &= \frac{1}{\pi}[2\phi + \sin\phi - \sin 2\phi - \tfrac{1}{3}\sin 3\phi]. \end{aligned}\right\} \tag{22}$$

Following Collins (1961) the coefficients R_k are found to be

$$R_k = -\frac{2\sqrt{2}}{\pi}\int_0^{\phi} F(u)\frac{\cos^3(\frac{1}{2}u)}{\sin u}\frac{\mathrm{d}}{\mathrm{d}u}\left[\frac{\cos(k+\frac{1}{2})u}{\cos\frac{1}{2}u}\right]\mathrm{d}u, \tag{23}$$

where

$$F(u) = \frac{\mathrm{d}}{\mathrm{d}u}\int_0^u \frac{\tan\frac{1}{2}\theta\sin^2\theta\cos\theta}{(\cos\theta-\cos u)^{\frac{1}{2}}}\mathrm{d}\theta. \tag{24}$$

After some rather tedious algebra the following explicit expression is obtained:

$$\left.\begin{aligned} R_k &= -\frac{1}{\pi}\left\{4[\cos(k+1)\phi + \cos k\phi](\tfrac{1}{2} - \tfrac{4}{3}\sin^2\tfrac{1}{2}\phi)\sin\phi \right.\right. \\ &\quad \left.\left. -2\left[\frac{\sin(k+3)\phi}{k+3} + \frac{\sin(k-2)\phi}{k-2}\right]\right\} \quad (k \neq 2), \\ R_2 &= -\frac{1}{\pi}\{4[\cos 3\phi + \cos 2\phi][\tfrac{1}{2} - \tfrac{4}{3}\sin^2\tfrac{1}{2}\phi]\sin\phi \\ &\quad -\tfrac{2}{5}\sin 5\phi - 2\phi\}. \end{aligned}\right\} \tag{25}$$

The difference between the shear stresses in the dispersed phase along the cap region as given by (11a,b) is

$$\frac{1}{\sin\theta}\frac{\partial}{\partial r}\left[\frac{1}{r^2}\frac{\partial}{\partial r}\left(\psi^{(2)} - \frac{\mu_1}{\mu_2}\psi^{(1)}\right)\right]_{r=1} = 2\left(1+\frac{\mu_1}{\mu_2}\right)\{h(\theta) + Re\,\tfrac{1}{8}A[h(\theta)+g(\theta)]\}, \tag{26}$$

where

$$\left.\begin{aligned} h(\theta) &= -\frac{\mu_2}{\pi(\mu_2+\mu_1)}\tan\tfrac{1}{2}\theta\left\{\tfrac{3}{2}(1+\cos\theta)\left[\sin^{-1}\left(\frac{\cos\theta-\cos\phi}{1+\cos\theta}\right)^{\frac{1}{2}}\right.\right. \\ &\quad \left.\left. + \frac{(\cos\theta-\cos\phi)^{\frac{1}{2}}(1+\cos\phi)^{\frac{1}{2}}}{1+\cos\theta}\right] + \frac{(1+\cos\phi)^{\frac{3}{2}}}{(\cos\theta-\cos\phi)^{\frac{1}{2}}}\right\}, \\ g(\theta) &= \frac{E}{\pi}\tan\tfrac{1}{2}\theta\left\{(1+\cos\theta)\left[\frac{(\cos\theta-\cos\phi)^{\frac{1}{2}}(1+\cos\phi)^{\frac{1}{2}}}{1+\cos\phi}\cos\theta\right.\right. \\ &\quad + \sin^{-1}\left(\frac{\cos\theta-\cos\phi}{1+\cos\theta}\right)^{\frac{1}{2}}\cos\theta \\ &\quad \left.\left. + \frac{(\cos\theta-\cos\phi)^{\frac{1}{2}}(1+\cos\phi)^{\frac{3}{2}}}{(1+\cos\theta)^2}\tfrac{1}{3}(2\cos\theta+5)\right] \right. \\ &\quad \left. + \frac{1}{3}\frac{(1+\cos\phi)^{\frac{3}{2}}}{(\cos\theta-\cos\phi)^{\frac{1}{2}}}(4\cos\phi-1)\right\}. \end{aligned}\right\} \tag{27}$$

Here the leading term was previously given by Sadhal & Johnson (1983) who pointed out the presence of a square-root singularity at $\theta = \phi$. However, as later shown by Sadhal & Johnson (1986) and also noted by Davis (1983) the total normal stress is

non-singular. Interestingly, this type of behaviour persists in the $O(Re)$ term. The analytical solution to $O(Re)$ also gives the correction for the drag. The general expression for drag force, F, is

$$F = 4\pi\mu_2 U R\left\{-\frac{2\mu_2+3\mu_1}{2\mu_2+2\mu_1}-\frac{\mu_2}{4(\mu_2+\mu_1)}C_1+S_1(Re) + Re\tfrac{1}{8}A\left[-\frac{2\mu_2+3\mu_1}{2\mu_2+2\mu_1}-\frac{\mu_2}{4(\mu_2+\mu_1)}C_1+\tfrac{1}{4}E R_1\right]\right\}+O(Re^2), \quad (28)$$

where analytical expressions for C_1 and R_1 are given by (22) and (25), respectively. The effect of the soluble surfactant is represented by the term S_1 and by E and A which also contain S_1. Therefore, when only the insoluble impurity is present, we may set $S_1 = 0$ and we have a fully analytical expression for F. For the general case, however, the calculation of the set of coefficients $\{S_k\}$ requires the numerical solution of the mass convection–diffusion equations. A standard finite-difference formulation is carried out to calculate the surfactant distribution in the drop and in the infinite continuous phase. A variable-size grid was employed in the radial direction with high concentration of grid points near $r = 1$. Thirty grid points were used in the radial direction in each phase. A common difficulty with this problem is that the surfactant wake behind the drop reaches the numerical outer boundary rather quickly with increasing Péclet numbers. This inconvenience can be overcome by increasing the outer-limit radius such that the wake vanishes before reaching the boundary. But there are two major disadvantages of this process: one is the increased c.p.u. time and the other is the higher instability levels at large radii. Therefore, an outer perturbation solution (see Acrivos & Taylor 1962)

$$c = e^{\frac{1}{2}\rho\cos\theta}\left(\frac{\pi}{\rho}\right)^{\frac{1}{2}}\sum_{k=0}^{\infty} A_k K_{k+\frac{1}{2}}(\tfrac{1}{2}\rho) P_k(\cos\theta) \quad (29)$$

was used for the far-field boundary condition. Here $K_{k+\frac{1}{2}}(\frac{1}{2}\rho)$ is the modified Bessel function of the second kind and ρ is the outer solution variable given by $\rho = Pe\, r$. This technique of satisfying a far-field boundary condition has been used before by Dennis, Walker & Hudson (1973). The matching is done at large values of ρ where

$$K_{k+\frac{1}{2}}(\tfrac{1}{2}\rho) \approx \left(\frac{\pi}{\rho}\right)^{\frac{1}{2}} e^{-\rho/2}. \quad (30)$$

By equating the mass fluxes and concentrations at the far-field numerical boundary and using (29), the series may be eliminated and one obtains

$$\frac{1}{Pe}\frac{\partial c}{\partial r} = \left[\tfrac{1}{2}(\cos\theta - 1) - \frac{1}{\rho}\right]c \quad (31)$$

The above condition is applied at 3–4 radii from the origin. The concentration profile is observed to be mostly uniform except in a narrow region near the rear axis.

The surface concentration Γ is then obtained from (13) and its derivative is taken numerically to calculate the right-hand side of (21). For cases with $\phi = 0$, (21) is integrated with respect to θ. A collocation procedure was used to calculate the set of coefficients $\{S_k\}$. The iteration is stopped when the differences between consecutive solutions for c and S_k are sufficiently small. The maximum number of terms that one can keep in the series is found to be 40. Beyond that limit it appears that the roundoff error becomes dominant. It is observed that the system becomes numerically

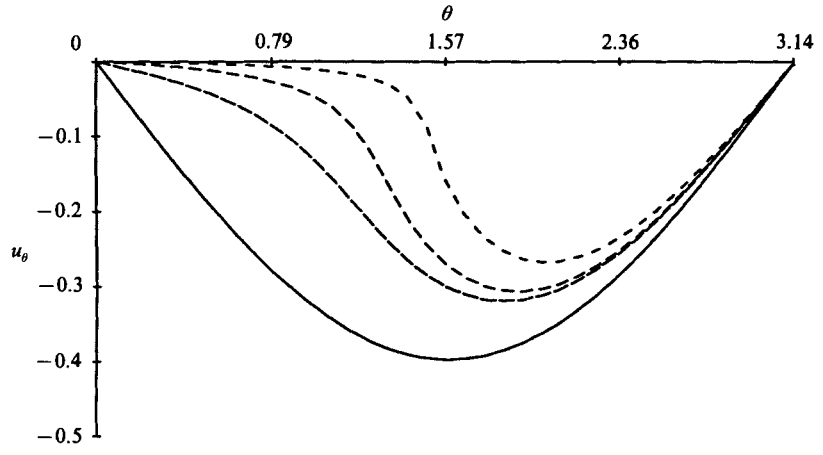

FIGURE 2. Interfacial velocity profile for soluble impurity only. $K = 0.5$, $E\ddot{o} = 30$, $\mu_1 = 0.2\mu_2$, $\beta = 1$, $Pe_2 = Pe_1$. ——, $Pe = 5$; ——, 50; —, 200; ---, 1000.

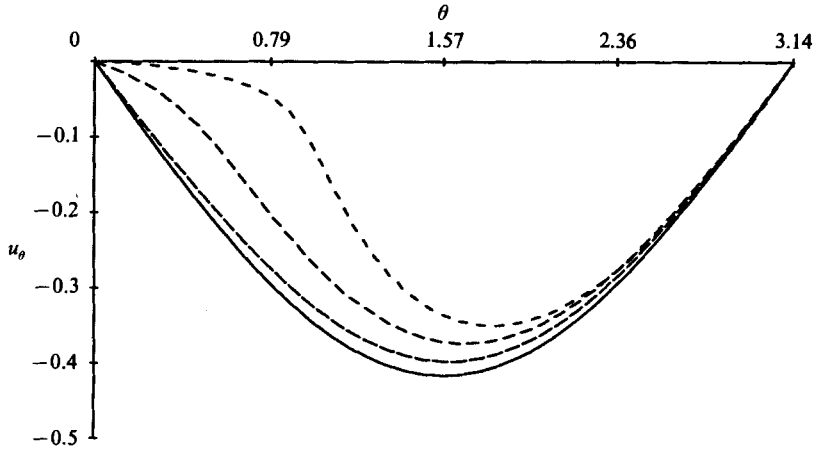

FIGURE 3. Interfacial velocity profile for soluble impurity only. $K = 0.05$, $E\ddot{o} = 30$, $\mu_1 = 0.2\mu_2$, $\beta = 1$, $Pe_2 = Pe_1$. ——, $Pe = 5$; ——, 100; —, 500; ---, 3500.

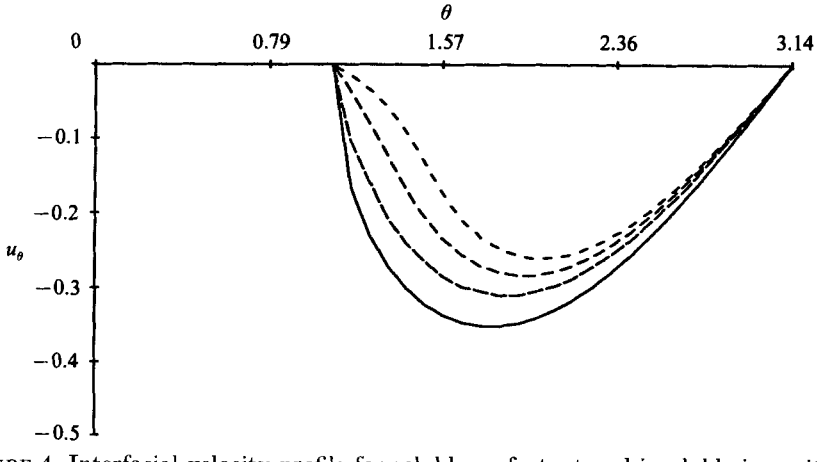

FIGURE 4. Interfacial velocity profile for soluble surfactant and insoluble impurity. $K = 0.1$, $E\ddot{o} = 30$, $\mu_1 = 0.2\mu_2$, $\beta = 1$, $Pe_2 = Pe_1$, $\phi = \frac{1}{3}\pi$. ——, $Pe = 5$; ——, 50; —, 200; ---, 600.

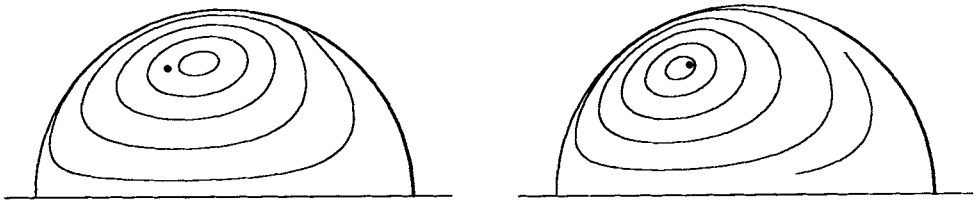

FIGURE 5. Streamlines in the drop: (*a*) insoluble impurity only, $Pe = 0$; (*b*) insoluble impurity and soluble surfactant, $Pe = 700$. $K = 0.1$, $E\ddot{o} = 30$, $\mu_1 = \mu_2$, $\beta = 1$, $Pe_2 = Pe_1$, $\phi = \frac{1}{3}\pi$. The solid circle ● indicates Horton's (1960) measurement for the same cap angle.

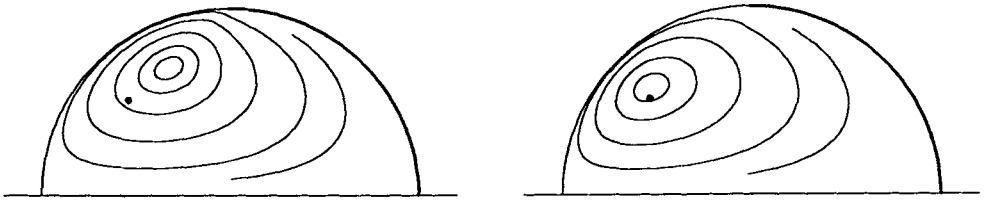

FIGURE 6. Streamlines in the drop: (*a*) insoluble impurity only, $Pe = 0$; (*b*) insoluble impurity and soluble surfactant, $Pe = 700$. Here $K = 0.1$, $E\ddot{o} = 30$, $\mu_1 = \mu_2$, $\beta = 1$, $Pe_2 = Pe_1$, $\phi = \frac{1}{2}\pi$. The solid circle ● indicates Horton's (1960) measurement for the same cap angle.

unstable with increasing values of K and Pe. The maximum value of the Péclet number where a stable solution can be obtained is affected greatly by K which represents the interfacial convection. In the next section the interfacial velocity profile is examined. This velocity profile gives important information about the behaviour of the cap.

4. Results and discussion

The plots of the interfacial velocity profile show that the interface in the back region of the drop slows down considerably with increasing Péclet number. In figure 2 the velocity profile along the interface is given for various values of the Péclet number. In this case only the soluble impurity is present and there is diffusion in both the bulk phases. The flow is taken to be in the Stokes regime. For high Péclet number, the interfacial velocity is nearly zero over a significant portion of the rear. In figure 3 a similar plot is given but here $K = 0.05$ is smaller than in figure 2. It is evident that much higher Péclet numbers are needed to achieve similar stagnation levels in the rear.

For cases in which both a soluble and an insoluble impurity is present, a distinct stagnant cap is formed. This is primarily due to insoluble impurity collecting in rear. In figure 4 the interfacial velocity profile is given for one case. The velocity reduction with Pe in the mobile region is similar to the single-impurity cases discussed before. The interesting aspect of the results is exhibited in the flow streamlines. The centre of the internal vortex shifts towards the front with increasing cap angle. This has been known earlier (see Sadhal & Johnson 1983). However, the theoretical treatments with only the insoluble impurity do not quite agree with Horton's (1960) experiments which provide data on the vortex centre position for

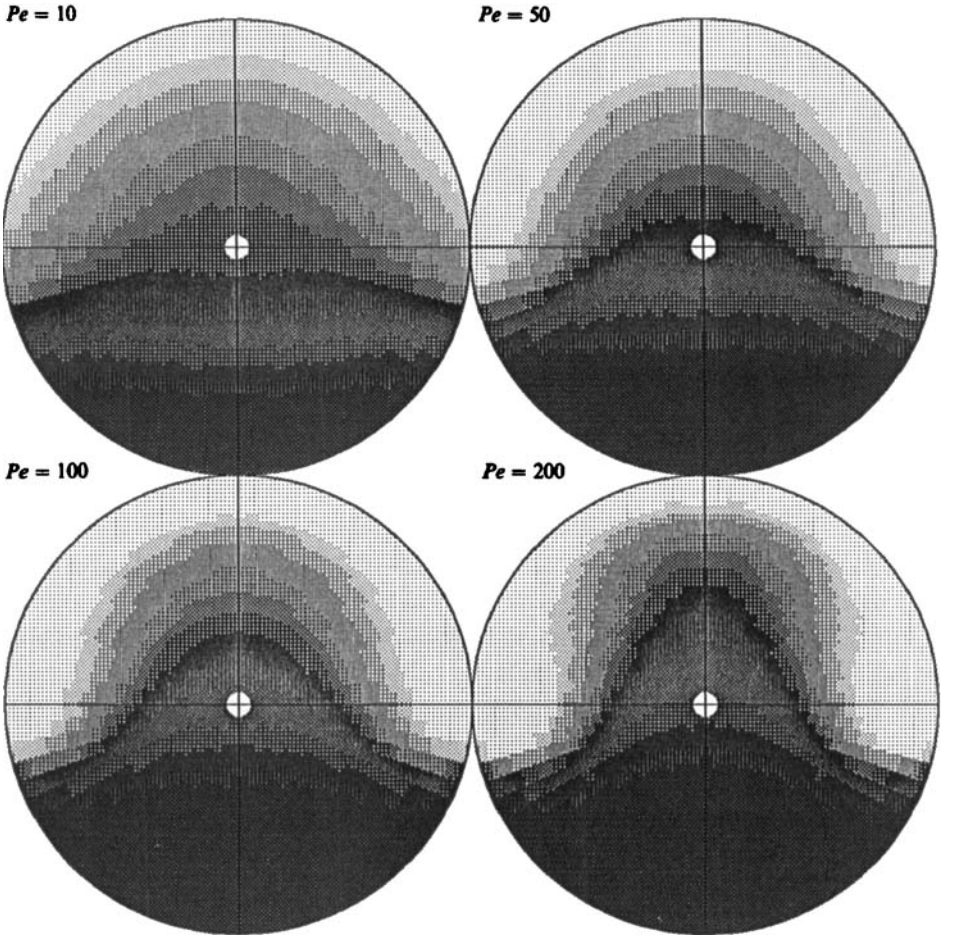

FIGURE 7. Concentration profiles in the drop for $K = 0.5$, $E\ddot{o} = 30$, $\mu_1 = 0.2\mu_2$, $\beta = 1$, $Pe_2 = Pe_1$.

various values of the cap angle. The theoretical work of Sadhal & Johnson (1983) as well as that of Harper (1982) underpredict the shifting, especially when a comparison is made for large cap angles. This disagreement has motivated the present analysis in which two impurities have been taken into consideration.

Comparison of the streamlines for cases with and without the soluble impurity has been made in figures 5 and 6. From these figures it is clear that the presence of the soluble surfactant in addition to the insoluble impurity further shifts the centre of the vortex. For sufficiently large Péclet number, agreement with Horton's (1960) experimental results is found. For example, in cases of a cap angle of $\phi = \frac{1}{2}\pi$ and $\phi = \frac{1}{3}\pi$, it can be seen in figure 6 that the experimental measurements of the centre of the vortex almost coincide with the theoretical prediction. It should be noted that Sadhal & Johnson (1983) showed that the internal circulation flow pattern is independent of the viscosity ratio when there is just the insoluble impurity. This has also turned out to be the trend for the present problem when both the soluble and the insoluble impurities participate in the fluid mechanics. It is therefore quite legitimate to compare the current theory with Horton's (1960) data without having to consider viscosities. However, the possible effects of a soluble impurity in addition

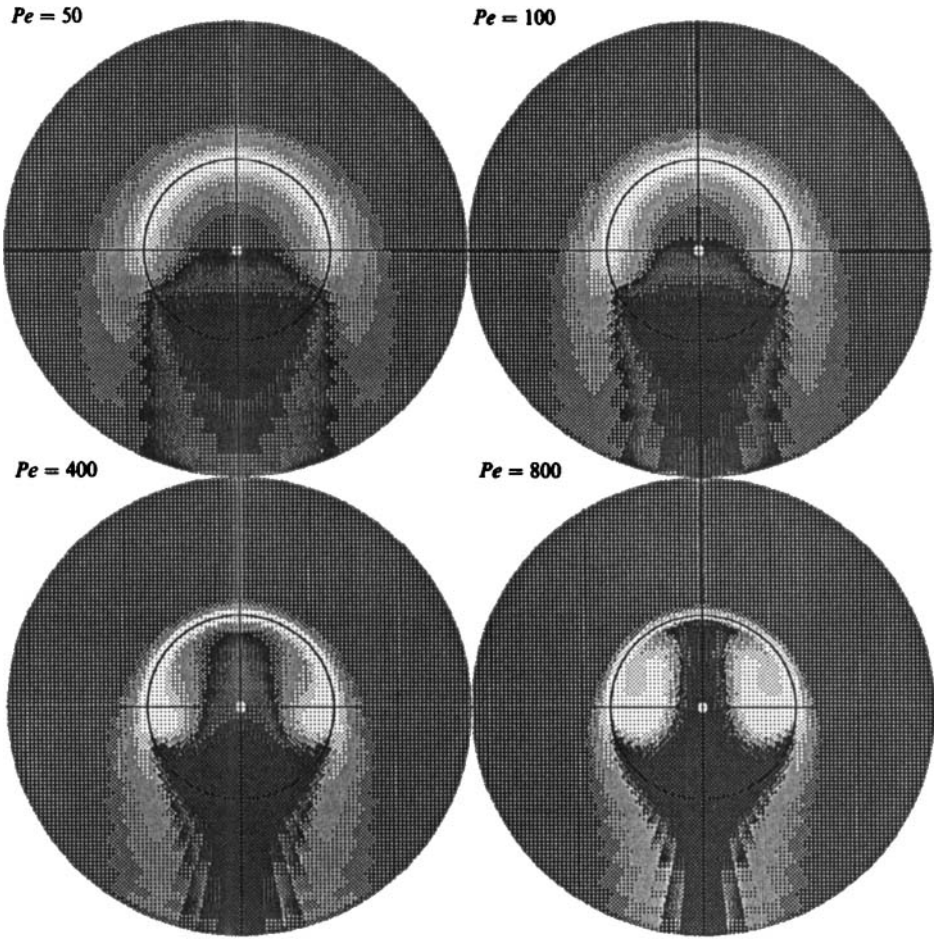

FIGURE 8. Concentration profiles for $K = 0.5$, $E\ddot{o} = 30$, $\mu_1 = 0.2\mu_2$, $\beta = 1$, $Pe_2 = Pe_1$.

to the particulate impurity were not considered in the experiments. Hence Péclet numbers for the experimental data are not available. Nevertheless, the present theory offers a meaningful explanation of earlier discrepancies.

The concentration distribution within the dispersed and the continuous phases has been obtained for various cases when only the soluble impurity is present. These are exhibited as pixel plots in figures 7, 8 and 9. The darker regions indicate higher concentrations. Figure 7 corresponds to diffusion in the dispersed phase only. The effect of internal circulation in transporting the surfactant towards the front is seen with increasing Péclet number. In figure 8 the surfactant is soluble in both the phases. For the high Péclet number the convective effects are evident from the elongation of external and the internal concentration wakes. In these two cases (figures 7 and 8) the constant K for surface kinetics of adsorption is taken to be 0.5, which may be considered to be rather large. In figure 9 K is taken to be 0.05. This results in a much weaker adsorption and the surface concentration tends to be lower. Similar surface retardation effects as for $K = 0.5$ are only achieved at much higher Péclet numbers: the effect of strong convective motion can be seen in figure 9 where $Pe = 3000$. Here, the surfactant is transported from the rear to the front by internal circulation giving rise to a high-concentration region around the front stagnation

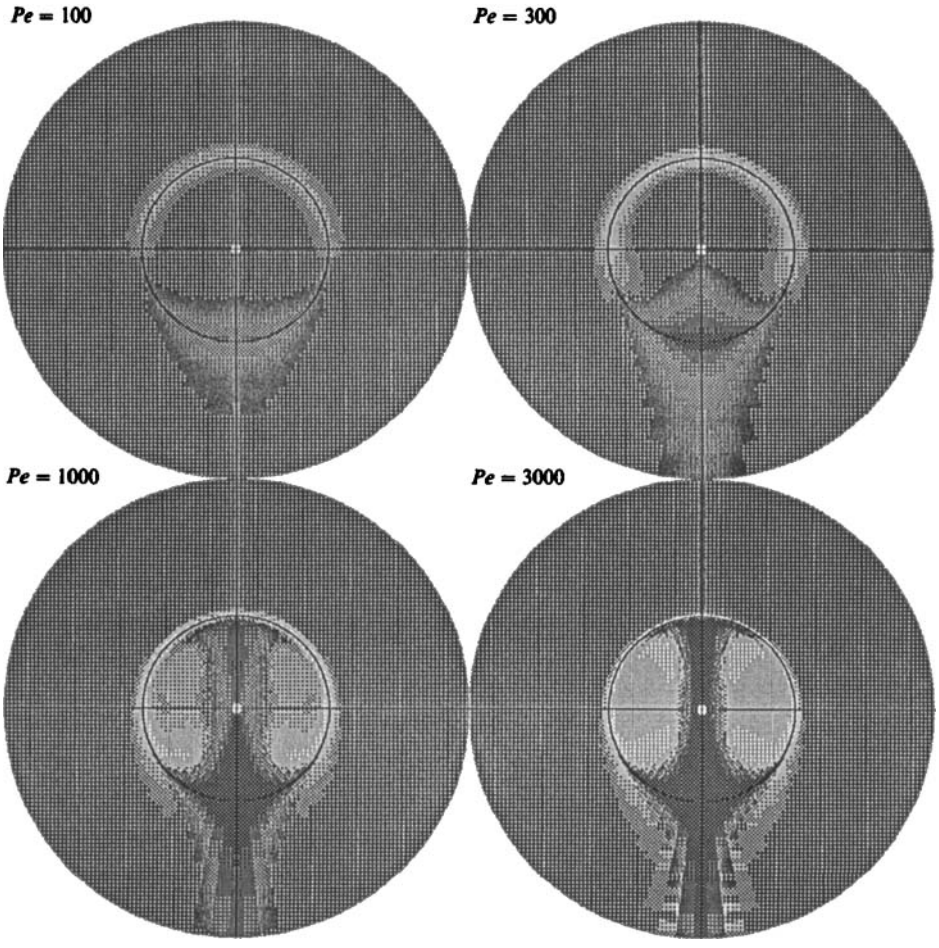

FIGURE 9. Concentration profiles for $K = 0.05$, $E\ddot{o} = 30$, $\mu_1 = 0.2\mu_2$, $\beta = 1$, $Pe_2 = Pe_1$.

point. This high concentration, however, does not greatly affect the continuous phase around that region. The primary reason for this behaviour is that the surface phase around the front stagnation point is virtually washed away by surface convection. As a result, the bulk concentration tends to be of proportional magnitude (equation (12)).

5. Conclusion

The current analysis is the first reported treatment of the effect of a surfactant on droplet motion with mass diffusion in both the dispersed and the continuous phases. Also, the simultaneous treatment of an insoluble impurity along with a soluble one has been carried out here.

The solution procedure required an analytical solution of the flow field with a Proudman–Pearson (1957)-type correction for the intertial effects. This, in fact, led to a fully analytical solution for the case when only the insoluble impurity is present. As a result, a correction to include inertia for the drag result of Sadhal & Johnson

(1983) has been given. When both the impurities were present, the analytical flow-field solution was generalized to be coupled with the soluble-surfactant transport. The equations for the latter process were solved numerically.

Since earlier theories on drop retardation could not adequately agree with experimental data, the idea of dealing with two impurities was proposed. It is theorized here that the distinct stagnant cap on the rear of the drop is the result of an insoluble impurity and that further retardation of interfacial velocities may be due to a soluble surfactant. This idea seems to be supported by experiments on the fluid dynamics of drop motion.

The authors are very grateful for the support of this work from the National Science Foundation (Grant No. CBT-83-51432), USC Faculty Research and Innovation Fund, TRW Systems Inc. and the Ralph M. Parsons Foundation. This work was carried out at the University of Southern California as a portion of the first author's doctoral dissertation.

Appendix

The leading-order solution to the Navier–Stokes equation for small Re is the Stokes solution that can be written as

$$\psi = \frac{1}{4}\left(2r^2 - Ar + \frac{B}{r}\right)\sin^2\theta. \tag{A 1}$$

This one-term Stokes solution can be written in terms of Oseen variable $\rho = Re\, r$ up to two terms as

$$2-\text{Oseen}\,(1-\text{Stokes})\,\psi = \frac{1}{2}\frac{1}{Re^2}\rho^2\sin^2\theta - \frac{A}{4}\frac{1}{Re}\rho\sin^2\theta. \tag{A 2}$$

Therefore, the Oseen expansion must have the form

$$\psi \approx \frac{1}{2}\frac{1}{Re^2}\rho^2\sin^2\theta + \frac{1}{Re}\psi_2(\rho,\theta), \tag{A 3}$$

where ψ_2 must satisfy the Oseen equation

$$\left(\mathrm{L}_{-1} - \cos\theta\frac{\partial}{\partial\rho} + \frac{\sin\theta}{\rho}\frac{\partial}{\partial\theta}\right)\mathrm{L}_{-1}\psi = 0. \tag{A 4}$$

A solution to this is $$\psi_2 = -2c_2(1+\cos\theta)[1-\mathrm{e}^{-\frac{1}{2}\rho(1-\cos\theta)}]. \tag{A 5}$$

Expanding this in terms of the Stokes variable up to one term gives

$$1-\text{Stokes}\,(2-\text{Oseen})\,\psi = \tfrac{1}{2}r^2\sin^2\theta - c_2\, r\sin^2\theta. \tag{A 6}$$

Therefore, $c_2 = \frac{1}{4}A$ to match the Oseen expansion (A 2) in Stokes variable

$$\psi \approx \tfrac{1}{2}r^2\sin^2\theta - \frac{A}{2Re}(1+\cos\theta)[1-\mathrm{e}^{-\frac{1}{2}Re\, r(1-\cos\theta)}]. \tag{A 7}$$

Expanding the two-term Oseen solution up to two terms in Stokes variable leads to

$$2-\text{Stokes}\,(2-\text{Oseen})\,\psi = \tfrac{1}{4}(2r^2 - Ar)\sin^2\theta + \frac{A}{16}Re\, r^2(1-\cos\theta)\sin^2\theta. \tag{A 8}$$

The Stokes expansion therefore must have the form

$$\psi \approx \frac{1}{4}\left(2r^2 - Ar + \frac{B}{r}\right)\sin^2\theta + Re\,\Psi_2(r,\theta), \tag{A 9}$$

where Ψ_2 must satisfy

$$\mathrm{L}_{-1}^2\,\Psi_2 = \frac{1}{r^2\sin\theta}\left(\psi_\theta\frac{\partial}{\partial r} - \psi_r\frac{\partial}{\partial\theta} + 2\cot\theta\psi_r - 2\frac{\psi_\theta}{r}\right)\mathrm{L}_{-1}\psi. \tag{A 10}$$

The general solution to the above equation is

$$\Psi_2 = C_2\left(2r^2 - A'r + \frac{B'}{r}\right)\sin^2\theta - \tfrac{1}{32}A\left(2r^2 - Ar - \frac{B}{r} + C + \frac{D}{r^2}\right)\sin^2\theta\cos\theta, \tag{A 11}$$

which is subject to certain boundary conditions. Now the two-term Oseen expansion of the two-term Stokes solution is

$$2-\text{Oseen}\,(2-\text{Stokes})\,\psi = \frac{1}{2}\frac{1}{Re^2}\rho^2\sin^2\theta + \frac{1}{Re}(2C_2\rho^2 - \tfrac{1}{16}A\rho^2\cos\theta - \tfrac{1}{4}A\rho)\sin^2\theta, \tag{A 12}$$

where $C_2 = \frac{1}{3}A$ to match (A 8).

REFERENCES

Acrivos, A. & Taylor, T. D. 1962 Heat and mass transfer from single spheres in Stokes flow. *Phys. Fluids* **5**, 387.

Agrawal, S. K. & Wasan, D. T. 1979 The effect of interfacial viscosities on the motion of drops and bubbles. *Chem. Engng J.* **18**, 215.

Bond, W. N. & Newton, D. A. 1927 Bubbles, drops, and Stokes law. *Phil. Mag.* **24**, 889.

Collins, W. D. 1961 On some dual series equations and their application to electrostatic problems for spheroidal caps. *Proc. Camb. Phil. Soc.* **57**, 367.

Davis, R. E. & Acrivos, A. 1966 The influence of surfactants on creeping motion of bubbles. *Chem. Engng Sci.* **21**, 681.

Davis, S. H. 1983 Contact-line problems in fluid mechanics. *Trans. ASME* E: *J. Appl. Mech* **50**, 977.

Dennis, S. C. R., Walker, J. D. A. & Hudson, J. D. 1973 Heat transfer from a sphere at low Reynolds number. *J. Fluid Mech.* **60**, 273.

Dukhin, S. S. & Deryagin, B. V. 1961 Kinetics of attachment of mineral particles to bubbles during flotation. V. Motion of the bubble surface strongly retarded by surface-active substances. Distribution of surface-active material and electric field of the bubble. *Russ. J. Phys. Chem.* **35**, 715.

Dussan V., E. B. 1982 Surface rheology. In *Proc. Ninth U.S. Natl Congress of Applied Mechanics, June 21–25, Ithaca, New York*, pp. 181–184.

Elzinga, E. R. & Banchero, J. T. 1961 Some observations on the mechanics of drops in liquid–liquid systems. *AIChE J.* **7**, 394.

Frumkim, A. N. & Levich, V. G. 1947 *Zh. Fiz. Khim.* **21**, 1183.

Garner, F. H. & Skelland, A. H. D. 1955 Some factors affecting droplet behaviour in liquid–liquid systems. *Chem. Engng Sci.* **4**, 149.

Griffith, R. M. 1962 The effect of surfactants on the terminal velocity of drops and bubbles. *Chem. Engng Sci.* **17**, 1057.

Harper, J. F. 1973 On bubbles with small immobile adsorbed films rising in liquids at low Reynolds numbers. *J. Fluid Mech.* **58**, 539.

Harper, J. F. 1982 Surface activity and bubble motion. *Appl. Sci. Res.* **38**, 343.

Holbrook, J. A. & LeVan, M. D. 1983*a* Retardation of droplet motion by surfactant. Part 1. Theoretical development and asymptotic solutions. *Chem. Engng Commun.* **20**, 191.

HOLBROOK, J. A. & LEVAN, M. D. 1983*b* Retardation of droplet motion by surfactant. Part 2. Numerical solutions for exterior diffusion, surface diffusion, and adsorption kinetics. *Chem. Engng Commun.* **20**, 273.

HORTON, T. J. 1960 M.S. Thesis, Illinois Inst. of Technology, Chicago.

HORTON, T. J., FRITSCH, T. R. & KINTNER, R. C. 1965 Experimental determination of circulation velocities inside drops. *Can. J. Chem. Engng* **43**, 143.

HUANG, W. S. & KINTNER, R. C. 1969 Effects of surfactants on mass transfer inside drops. *AIChE J.* **15**, 735.

LEVAN, M. D. 1981 Motion of a droplet with a Newtonian interface. *J. Colloid Interface Sci.* **83**, 11.

LEVAN, M. D. & NEWMAN, J. 1976 The effect of surfactants on the terminal and interfacial velocities of bubbles or drops. *AIChE J.* **22**, 695.

LUCASSEN, J. & GILES, D. 1975 Dynamic surface properties of nonionic surfactant solutions. *J. Chem. Soc. Faraday Trans.* **171**, 217.

NEWMAN, J. 1967 Retardation of falling drops. *Chem. Engng Sci.* **22**, 83.

POSKANZER, A. & GOODRICH, F. C. 1975 A new surface viscometer of high sensitivity, I. Theory, II. Experiments with Stearic acid monolayers. *J. Colloid Interface Sci.* **52**, 201.

PROUDMAN, I. & PEARSON, J. R. A. 1957 Expansions at small Reynolds numbers for the flow past a sphere and a circular cylinder. *J. Fluid Mech.* **2** 237.

SADHAL, S. S. & JOHNSON, R. E. 1983 Stokes flow past bubbles and drops partially coated with thin films. Part 1. Stagnant cap of surfactant film – exact solution. *J. Fluid Mech.* **126**, 237.

SADHAL, S. S. & JOHNSON, R. E. 1986 On the deformation of drops and bubbles with varying interfacial tension. *Chem. Engng Commun.* **46**, 97.

SAVIC, P. 1953 Circulation and distortion of liquid drops falling through a viscous medium. *Nat. Sci. Res. Council Can. Div. Mech. Engng Rep.* MT-22.

SAVILLE, D. A. 1973 The effect of interfacial tension gradients on the motion of bubbles or drops. *Chem. Engng J.* **5**, 251.

SCHECHTER, R. S. & FARLEY, R. W. 1963 Interfacial tension gradients and droplet behaviour. *Can. J. Chem. Engng* **41**, 103.

SCRIVEN, L. E. 1960 Dynamics of a fluid interface. Equation of motion for Newtonian surface fluids. *Chem. Engng Sci.* **12**, 98.

SLATTERY, J. C., CHEN, J., THOMAS, C. P. & FLEMING, P. D. 1980 Spinning drop interfacial viscometer, *J. Colloid Interface Sci.* **73**, 483.

WASSERMAN, M. L. & SLATTERY, J. C. 1969 Creeping flow past a fluid globule when a trace of surfactant is present. *AIChE J.* **15**, 533.

VAN DYKE 1975 *Perturbation Methods in Fluid Mechanics.* Parabolic.